Production of strongly coupled plasmas by the laser irradiation of thin metallic films confined within micrometer-scale gaps by transparent insulators

G. R. Bennett, J. S. Wark, D. J. Heading, N. C. Woolsey, and H. He
Department of Physics, Clarendon Laboratory, University of Oxford, Parks Road, Oxford, OX1 3PU, United Kingdom

R. Cauble, R. W. Lee, and P. Young
Lawrence Livermore National Laboratory, Livermore, California 94550
(Received 24 May 1994)

A method of producing strongly coupled plasmas by the laser irradiation of thin metallic foils is described. The foils are deposited on the inside surfaces of two crystals placed parallel, and spaced by a few-micrometer gap. Laser irradiation of the foils through the transparent confining walls creates a plasma with a Coulomb interaction potential similar in magnitude to the kinetic energy. Use of *X*-cut quartz as the confining material allows direct measurement of the plasma pressure. The lifetime of the plasma is typically more than an order of magnitude longer than the laser pulse for incident pulses of nanosecond duration. The target design appears promising for the measurement of several plasma characteristics such as the equation of state, Coulomb logarithms, and transport coefficients, and the resultant plasma conditions compare favorably with those produced by methods based on x-ray heating of confined metallic foils requiring laser energies that are larger by several orders of magnitude.

PACS number(s): 52.50.Jm, 52.25.−b, 52.55.−s

I. INTRODUCTION

Strongly coupled plasmas are those which exhibit Coulomb interaction energies comparable to or greater than the kinetic energy, i.e., the coupling parameter Γ is greater than unity, where $\Gamma=(Z^*e)^2/rk_BT$. Here r is average the ion separation, Z^* the effective ion charge, and T the temperature. The properties of such plasmas, including their equations of state and transport coefficients, are predicted to deviate significantly from those of classical plasmas. Several methods have previously been put forward for the production and measurement of plasma properties, such as capillary discharges [1], exploding wires [2], and strongly shocked solids and gases [3,4].

Hot, dense plasmas have also been generated by pulsed x-ray heating of thin foils sandwiched between plastic tampers [5], where the x-ray pulse is produced by the laser irradiation of a high Z target. Using the measured x-ray flux from a Au burn-through foil one can determine the behavior of the sample [5]. As an example we show calculations of the conditions reached in a thin foil of Teflon, CF_2, tamped with a plastic, CH, layer. The dimensions of the sample are 2000 Å of CH on either side of a 1400 Å CF_2 foil. Using the volumetric heating provided by the x rays from the Au burn-through foil, the sample expands, holding the central region at a uniform high density.

In Fig. 1 we show the results of a simulation performed using the HYADES one-dimensional hydrodynamics code with the appropriate x-ray flux. The effective dilution of the x-ray flux due to the stand off of the x-ray source from the foil is included in the calculation. The time dependence of the central portion of the Teflon layer is shown in the figure. The calculation shows that the peak temperatures reached are of the order of 16 eV when the electron density is 10^{21} cm^{-3}. It is important to note that the creation of the x-ray source is achieved with less than 10% of the laser energy up converted into the x-ray source. The x-ray deposition in the thin sample indicates the coupling efficiency is less than 10%. Finally, the fact that one desired hydrodynamic isolation demands that the source be removed from the sample leads to a further dilution leaving approximately 10% of the source energy to impinge on the sample. Here we have taken the source to be a 1 mm square at a distance of 3 mm from the center of the tamped sample. These factors lead to an estimate of the coupled energy of the laser originally impinging on the Au foil of less than 0.001, thus requiring the use of multikilojoule lasers for this method of plasma

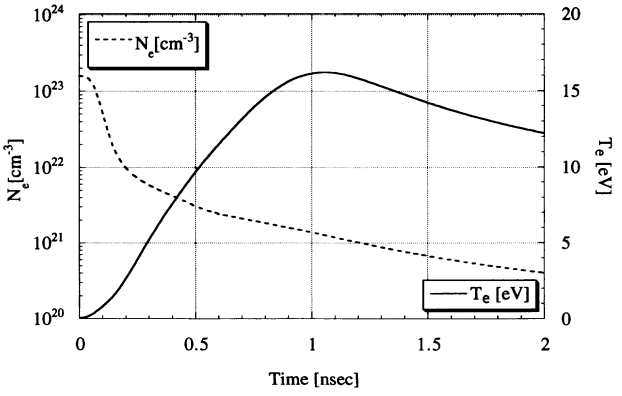

FIG. 1. History of plasma conditions predicted by the HYADES hydrodynamic code for the conditions of a thin Teflon foil irradiated by a pulse of x rays from a remote, separate, laser-heated Au target (details given in the text).

creation, although less energy can be used if less stringent requirements are made on the uniformity of the plasma [6].

Such methods have been used to investigate the opacity of the plasma in regions of astrophysical interest [7]. As stated above, the main disadvantage of this method of plasma production is that it requires the use of very large laser systems due to the inefficiency of conversion of laser light to plasma thermal energy via the x rays. The development of simpler methods of production of hot dense matter, where the plasma is accessible to probing and diagnosis, is therefore of considerable importance. We present here a method of production of hot (>15 eV) dense ($\sim 1\%$ solid) matter than requires considerably less laser energy (~ 1 J), and yet allows the extraction of information concerning the density and pressure directly, and in principle is amenable to probing techniques. It is based on a extension of the concept of confined laser ablation [8–15].

In this mode of laser-matter interaction, the absorbing (usually metallic) target is placed in intimate contact with a transparent overlaying material, as shown in Fig. 2(a). The short (nanosecond) pulse of laser light is incident on the transparent material at an irradiance below its breakdown threshold (typically 10^{10}–10^{11} W cm^{-2}). The light thus passes through the overlay and produces a plasma at the metallic surface. This plasma is inertially confined between the transparent overlay and the bulk of the metallic target. It expands, launching a shock wave of typically tens of kbar into the confining materials. The plasma conditions are thought to start at densities close to solid, with temperatures ranging from below 1 eV up to approximately 10 eV. Owing to the rapid expansion, the plasma conditions (i.e., pressure, density, and temperature) initially change rapidly on a nanosecond time scale.

A further related method of laser producing strongly coupled plasmas has recently been suggested by Mayer and Bush [16]. It is shown schematically in Fig. 2(b). In this method the transparent substrate is coated on one side with a thin metallic film, and the laser beam once again vaporizes the film by irradiation through the transparent substrate. In contrast to the confined ablation method the plasma is now allowed to expand freely into the surrounding vacuum. Mayer and Bush have shown that the expansion of the vapor is predominantly one dimensional and supersonic ($M \sim 10$). Mostoyvich *et al.* have allowed such a laser-produced vapor to pass through slits, reheated it with a separate laser beam, and measured the inverse bremsstrahlung absorption of the resultant strongly coupled plasma, and thus the effective Coulomb logarithm [17]. The main errors in their measurements arise from the density gradients present in the plasma.

In distinction to these methods we present here an extension of these two ideas to a form of confined laser ablation, where the laser-irradiated confined metallic foil is produced within a predefined micrometer-scale gap. This method was first proposed by Yang [8], but this work represents an application of this technique. It is shown schematically in Fig. 2(c). It is demonstrated that this method produces plasmas that are relatively long lived (they last up to an order of magnitude longer than the laser pulse), are dense (of order 1% of solid), and hot (up to 15 eV). If a thin (few hundred Å) metallic film is employed such that complete vaporization of the film occurs, we have the added advantage of a good knowledge of the ion density simply from the initial foil and gap thicknesses. It is shown below that if a piezoelectric crystal (such as *X*-cut quartz) is used as the rear confining wall, the pressure of the plasma can be determined directly by monitoring this piezoelectric

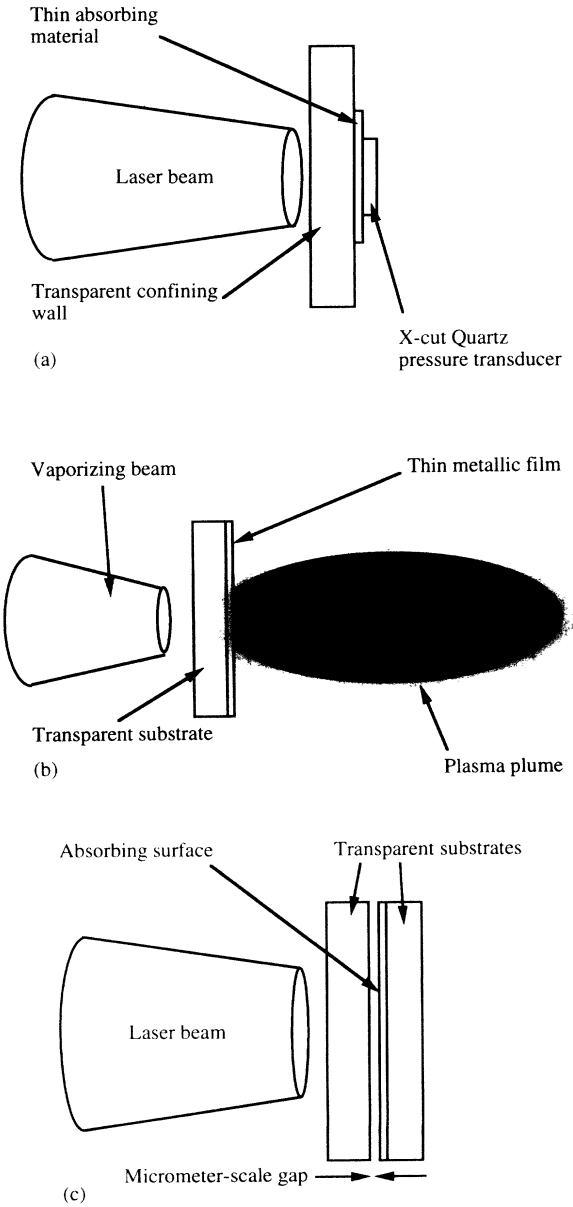

FIG. 2. A schematic diagram of the target design for confined laser ablation where (a) the absorbing surface is in intimate contact with the transparent confining wall; (b) where the absorbing film, irradiated from the side that is in contact with a transparent plate, is allowed to expand into the vacuum; and (c) irradiation of metallic foils which subsequently expand into a predefined micrometer-scale gap.

response. With a knowledge of the ion density, the peak plasma pressure, and the energy deposited in the plasma, we can extract information about the equation of state of the plasma, and compare it to theoretical models, as long as thermal losses from the plasma to the confining walls are small. We shall show that thermal losses are small at high laser irradiances (and hence higher pressures, 20–35 kbar), but start to become important at low (<20 kbar) pressures. The data are consistent with a simple model that assumes that the surfaces of the quartz confining walls melt, and that the energy lost to them is roughly constant. Thus a larger fraction of the energy is lost the lower the pressure. The good agreement at higher pressures (>20 kbar) indicates that in this regime we have created a plasma with a well-defined density, pressure, and internal energy which could therefore be used for the study of strongly coupled plasmas.

II. EXPERIMENTS

For the experiments described here both confining crystals were manufactured from X-cut quartz and polished flat to $\lambda/10$. The rear crystals were 2 cm in diameter and either 1 or 2 mm thick. The dimensions of the front crystal are shown in Fig. 3. The inner surfaces of the two crystals were coated with 80 Å (front disk) and 270 Å (rear disk) of aluminum. In addition, on the outer edge of the inner surface of the wedged front crystal, a 20 nm layer of chromium and then 3.5 μm copper spacers were deposited to produce the micrometer-scale gap. The two crystals were placed in contact, and held together by the clamping mechanism shown. The inner surfaces of the crystals were positioned to be parallel by adjusting the clamping screw, and the degree of parallelism of the surfaces was monitored by the observation of the interference fringes through the crystal coated with the semitransparent 80 Å layer. When the surfaces were parallel a single Newton's ring was observed over the whole crystal diameter. Errors in the degree of parallelism over the portion of the target to be laser irradiated

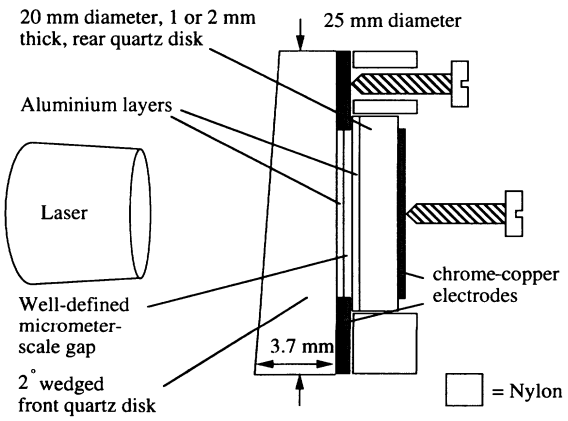

FIG. 3. A schematic diagram of the apparatus used to create the confined laser-produced plasma within a well-defined micrometer-scale gap.

were estimated from the range of colors present in this single ring. The gap spacing was measured by use of an interferometric method employing a green helium-neon laser. The laser was incident upon the center of the target at an angle of incidence, θ. As the target was rotated, altering the angle θ, the intensity of the reflected laser beam passed through maxima and minima due to interference between reflections from the metallic layers on either side of the gap, thus yielding the gap thickness. Typical gaps produced by this method were of order 3.5–7.0 μm, and could be measured with an accuracy of $\pm 5\%$.

The choice of metallic foil thickness was determined by the desire to produce a plasma with a well-defined ion density, thus requiring complete vaporization of the metallic foil by the incident laser. We have performed a series of experiments irradiating targets of different foil thicknesses while monitoring the optical (700 nm) emission from both sides of the irradiated target. For targets with foil thicknesses of 500 Å or less, similar levels of emission are observed on both sides of the target, whereas significant differences are found for thicknesses in excess of 1000 Å. These observations are consistent with measurements of the transmitted laser energy through the combined 80+270 Å layer, which show up to $\sim 10\%$ transmission for the intensity range of interest.

The rear surface of the double-crystal target was coated with a thin layer of chrome (20 nm) and copper (1000 nm) of 16 mm diameter. The short-circuit current between this electrode and that formed by the plasma in electrical contact with the spacers between the two crystals allowed the rear confining quartz crystal to be used as a pressure gauge [18–23]. The temporal response of this gauge over several microseconds was monitored with a Hewlett-Packard 1 giga-sample/sec digitizing oscilloscope with a bandwidth of 250 MHz and a risetime of 1.4 nsec: an analog oscilloscope of approximately double this speed simultaneously recorded the same signal over a time interval of 10 nsec. The peak pressures measured by the faster oscilloscope were found to be approximately 10% higher than those measured with the digitizing scope.

If we neglect losses to the quartz confining walls, which is discussed in more detail below, the internal energy change of the aluminum plasma is equal to the absorbed laser energy; this was obtained from calorimetry measurements of the incident, reflected, and transmitted laser energies. The transmitted energy and pressure could not be measured simultaneously because the rear electrode blocks laser light transmitted through the two aluminum layers. If this electrode reflected all laser light back into the plasma, then there would be no need to know its value; in fact such a perfect reflection would help to produce uniform heating of the plasma. If, however, a plasma forms at the rear electrode of comparable pressure to the confined aluminum plasma, then a large error in the measurement of the pressure of the confined plasma would occur since the piezoelectric current is proportional to the difference in applied stress between the two crystal surfaces. Measurements of the transmitted energy indicate that any plasma formed at this electrode has a

pressure $\ll 1$ kbar, which is much less than all measured peak pressures.

III. RESULTS

The experiments were performed at the Janus research laser of the Lawrence Livermore National Laboratory, and at the Vulcan laser of the Central Laser Facility of the Rutherford Appleton Laboratory. The target were irradiated with between 1 and 11 $J\,cm^{-2}$ of 1.053 μm laser light in pulse lengths ranging from 1 to 4 nsec [full width at half maximum (FWHM) Gaussian]. The resultant irradiances ($0.25-3.0\times10^{9}$ $W\,cm^{-2}$) were well below the breakdown threshold for quartz at these pulse lengths.

Typical data showing the pressure histories obtained from the quartz gauge are shown in Fig. 4 for three different peak pressures. We find that the plasma pressure increases approximately linearly to the peak over times of 4 and 6 nsec for laser pulses of 1 and 4 nsec duration, respectively. This linear pressure rise allows one to estimate the small increase in plasma volume and the work done in compressing the walls prior to peak pressure. For a 6 nsec risetime to a 4 kbar peak pressure the gap changes by 0.16 μm and the associated work done is 4.2×10^{-3} $J\,cm^{-2}$. Similarly, for a 36 kbar peak pressure, we estimate the gap increases by 1.4 μm and the work done compressing the quartz is 0.34 $J\,cm^{-2}$. Note that for the majority of the data presented here the peak pressure is below about 20 kbar, and the fractional increase in plasma volume due to compression of the confining walls prior to the peak of the pulse is less than 20%. After the peak, the pressure pulse decays with a $1/e$ decay time of typically 20 nsec, that is about an order of magnitude longer than the laser pulse. The decay of the pressure pulse will have several components: the expansion of the plasma; the associated work done in compressing the quartz; losses due to the latent heat of melting and vaporization of the quartz confining walls; and diffusion into the bulk of the quartz.

In the presentation of the results of the measured peak pressure, in a similar manner to the authors of previous work [8,15], we introduce the parameter α, where $\alpha=3P/2U$, and U is the internal energy per unit volume. Thus α gives us a measure of how much internal energy per unit volume is expressed as pressure, and the fraction that is used in ionization, vaporization, the overcoming of Coulombic attraction, and thermal diffusive losses. The results are shown in Fig. 5. We first compare these results for the peak pressure with predictions which ignore thermal losses to the confining walls. We will next estimate the approximate level of thermal losses, and proceed to show that the data are consistent with a simple model including diffusion.

If heat losses to the quartz are neglected, and the relatively small changes in plasma volume and work done prior to the peak of the pulse are accounted for, we can then directly compare the measured peak pressure, mass per unit volume, and internal energy per unit volume with those predicted by various equation of state models. The experimental data are compared in Fig. 5 with SESAME models [24,25], the first (table 3715) is based on a solution to the Saha-Boltzmann (SB) equation, while the second, from SESAME table 3717, is based on the Thomas-Fermi-Dirac (TFD) model. The predicted Γ value from table 3717, in conjunction with table 23714 (23714 for average ionization), is shown in Fig. 5(b) along with the predicted plasma temperature from table 3717 only. The shot-to-shot variation in gap thickness resulted in plasma densities in the range 0.46–0.98 % of solid, but SESAME indicates that this results in variations in α of order 10% for the pressure range of interest, significantly less than the error bars in the data. It can be seen that

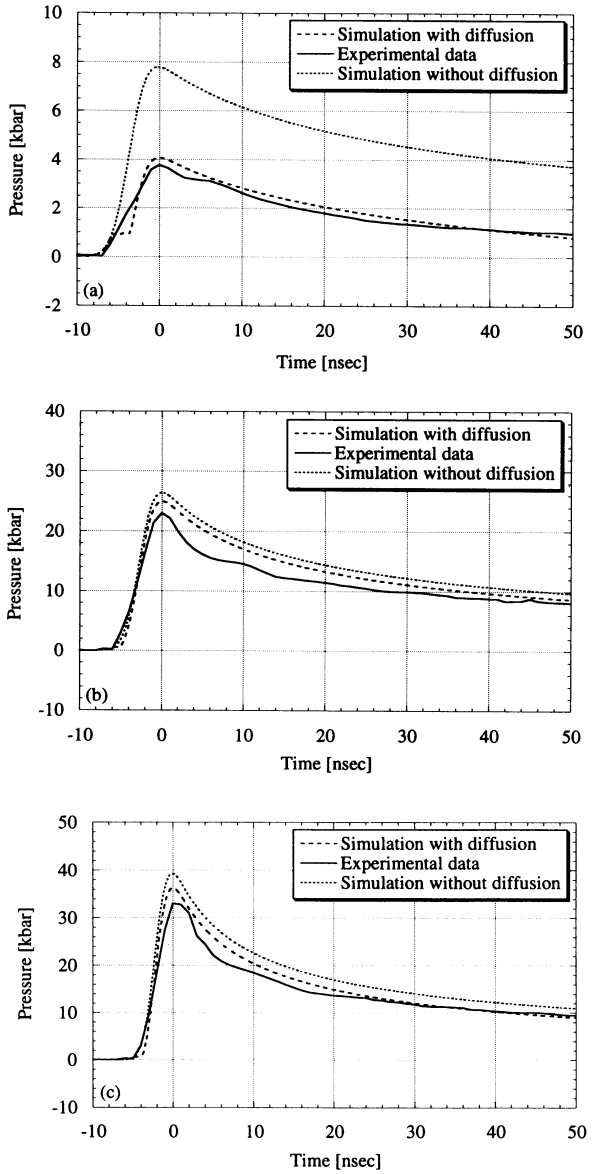

FIG. 4. The solid line shows the experimental results for the pressure histories for absorbed energies of (a) 1.25 $J\,cm^{-2}$, (b) 7.9 $J\,cm^{-2}$, (c) 10.1 $J\,cm^{-2}$ in a laser pulse of 4 nsec (FWHM). The dashed line shows the results from the diffusion model discussed in the text for values of $\beta\theta_m$ (in units of 10^7 $J\,m^{-2}\,s^{-1/2}$) (a) 2.49, (b) 4.0, (c) 8.0. In each case the dotted line shows the results of the model neglecting the effects of diffusion.

there is reasonable agreement, within the error bars of the experiment, with the TFD model predictions for pressures of 20–35 kbar, with values of α of order 0.4, corresponding to predicted values of the coupling parameter Γ greater than unity. We note that this value of α is significantly higher than that inferred from previous confined ablation experiments [8,15]. However, for lower pressures between 2 and 20 kbar, a significant departure from both SESAME models is found, with the values of α being up to approximately a factor of 2 less than those predicted at the lowest pressures measured. Even more severe discrepancies were reported by Fabbro *et al.* [15], and by other workers [8]; in each case the measured peak pressures were considerably less than those predicted. We believe that these differences are explained by energy loss from the plasma due to thermal diffusion.

Although there is little information about the thermal conductivity and diffusivity of materials at high temperatures, simple estimates show that a considerable fraction of the laser energy can be lost during the laser pulse by conduction into the quartz confining walls, and thus thermal losses should be considered in the modeling of the plasma pressure history. For example, within a time t we would expect the energy loss to be of order $4(\rho CKt/\pi)^{1/2}\bar{T}$ [25], where $\bar{T}$ is the melting temperature of the quartz, ρ the density, C the heat capacity, and K the thermal conductivity. Using values $C=1325$ J kg^{-1} K^{-1} [24,25], $\bar{T}=1883$ K, $\rho=2.65$ g cm^{-3}, and $K=3$ W m^{-1} K^{-1}: we find that at least 0.1 J cm^{-2} can be lost during the 6 nsec risetime of the peak pressure. The 36.3 kbar high pressure data shown in Fig. 3 are obtained with 10.1 J cm^{-2}, whereas the lower pressure data correspond to irradiances of 1.25 J cm^{-2}. Thus it can be seen that heat loss during the pulse can be a significant factor, especially for the lower pressure data. The observed peak pressures can be understood using a simple model which is an extension of that put forward by Fabbro *et al.* [15], but with the addition of a thermal diffusion term. We emphasize that the simple calculation of thermal losses given above should be treated as an estimate, as there is considerable uncertainty in the value of the diffusivity of quartz under these conditions, and in the simulations described below the value of the diffusivity is adjusted to give reasonable agreement with the data.

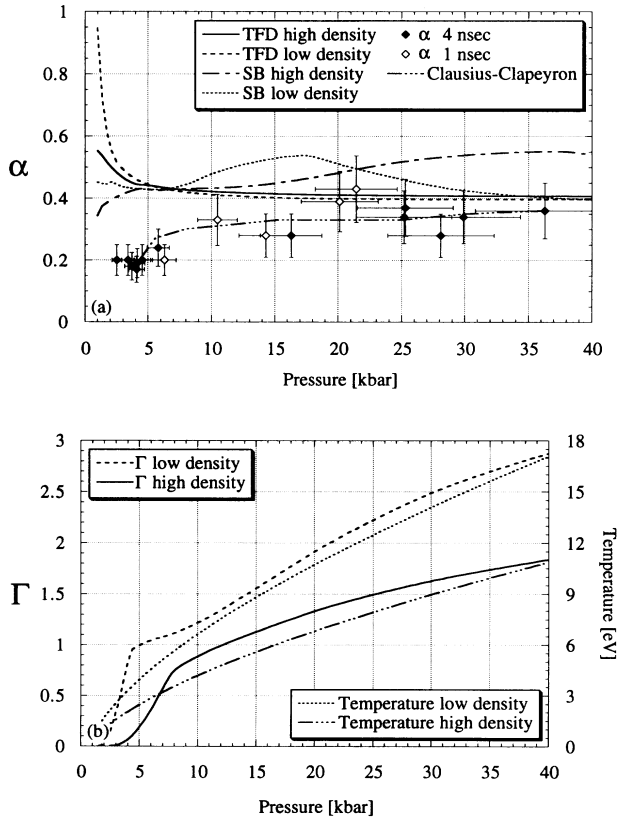

FIG. 5. (a) A comparison of the value of α deduced from the measured peak pressure, mass per unit volume, and absorbed energy per unit volume with that predicted from two of the tables of the SESAME equation of state. Also shown is the predicted peak pressure using the thermal diffusion model described in the text. In (b) is shown the predicted value of the coupling parameter Γ and the plasma temperature, assuming no thermal losses. High density refers to 0.98% solid density and low density refers to 0.46% solid density.

IV. SIMULATIONS

For the study of confined ablation where the absorbing plasma is in intimate contact with the confining overlay, Fabbro *et al.* [15] put forward a very simple model for predicting the pressure history of the plasma, which is easily extended to the situation described here, where we have a predefined gap into which the plasma expands. In this model they assume that α is constant throughout the expansion of the plasma, i.e.,

$$P(t)=\tfrac{2}{3}\alpha U(t)\ , \tag{1}$$

where $U(t)$ is the internal energy per unit volume of the plasma. The rate of change of plasma volume will depend on the plasma pressure and the impedance Z of the confining walls:

$$\frac{dL(t)}{dt}=\frac{2}{Z}P(t)\ . \tag{2}$$

And from Eq. (7) in Ref. [15] we see that the energy per unit area deposited by the laser in the time interval $t\rightarrow t+dt$ is given by

$$I(t)dt=P(t)\frac{dL(t)}{dt}dt+\frac{3}{2\alpha}\frac{d}{dt}[P(t)L(t)]dt\ . \tag{3}$$

To modify Eq. (3) to take into account diffusion we must make several simplifying assumptions. We first assume that until the surface of the confining wall reaches the melting temperature θ_m, heat loss from the plasma is negligible and, second, from the time of melting, t_m, we assume that the edge of the confining wall remains at this temperature. This allows us to modify Eq. (3) to

$$I(t)dt=P(t)\frac{dL(t)}{dt}dt+\frac{3}{2\alpha}\frac{d}{dt}[P(t)L(t)]dt+\beta\frac{\theta_m}{\sqrt{t'}}dt\ , \tag{4}$$

where $t'=t-t_m$, $\beta=0$ $(t'\leq 0)$, and β is a diffusion con-

stant for $t' > 0$ which we can vary to get agreement with the data.

Equations (2) and (3) have been solved computationally consistently with Eq. (4) using the experimentally determined specific pulse lengths and absorbed energy per unit area values. Figure 5 shows the weak pressure and density dependence of α; therefore a constant $\alpha = 0.4$ is used throughout. In each case the value of $\beta\theta_m$ has been adjusted to give the best fit with experimental data, and the results are shown alongside the experimental data in Fig. 4. It can be seen that in general there is good agreement, both with the peak pressures observed, and in the late time behavior of the pressure. Note that when diffusion is neglected the peak pressure of the low pressure shot approximately doubles, so giving an α of around 0.4.

It can be seen that the value of $\beta\theta_m$ for best fit with the experimental data increases with pressure. This is reasonable as $\bar{T}$ increases with pressure (for fixed density). We can estimate the pressure-dependent melting point by use of the Clausius-Clapeyron equation. Assuming the latent heat of melting is temperature independent ($L = 142$ kJ/kg), and the density of molten quartz is 2.2 g cm^{-3} (compared with 2.65 g cm^{-3} for solid quartz), then the average melting point during the expansion is given by

$$T(P) \approx T_m \exp\{P/(2B)\} , \tag{5}$$

where $T_m = 1883$ K is the melting point in vacuum, P is the peak pressure in kbar, and $B = 18.7$ kbar. Thus at 36 kbar we may expect the melting point to be approximately a factor of 2.7 greater than that at 4 kbar; this should be compared with the increase of a factor of $8/2.5 (= 3.2)$ in $\beta\theta_m$ found using the diffusion model, as described in Fig. 4, and is equivalent to an experimental value of B of 14.8 kbar. Note that care should be taken in making such comparisons using Eq. (5), as our model is assuming a constant, average melting point during the pressure pulse, whereas it will in practice be time dependent, and the above calculation serves to illustrate that an increase of $\beta\theta_m$ of the magnitude needed to obtain a fit to the higher pressure data is not unreasonable.

The observed peak pressures have been modeled using the above model. From the low (4 kbar) pressure value of $\beta\theta_m$ of 2.49×10^7 J m^{-2} s$^{-1/2}$ shown in Fig. 4(a) we obtain a value of β of 1.25×10^4, assuming the zero pressure value of the melting point. We then employ the pressure-dependent melting point outlined in Eq. (5) assuming the experimentally determined value of B. The results of these simulations are shown alongside the experimental data in Fig. 5. It can be seen that there is excellent agreement between this simple theory and experiment.

By using the simple diffusion model it is clear that a reasonable agreement between experiment and theory may be obtained. On the one hand, caution should be used in employing such a simple model because of course, in practice, the melting point and α will vary throughout the pressure pulse, and the loss of energy due to diffusion should really be modeled by a much more complicated model incorporating all of the significant physics, and a more sophisticated equation of state. On the other hand, this simple model serves to illustrate the plausibility of heat loss as the mechanism causing the reduction of pressure from that expected, and is useful for crude quantitative predictions. It is encouraging that such a simple model seems to explain the reduction in the peak pressures from those predicted if diffusion is neglected, and simultaneously explains the subsequent decay of the pressure pulse.

We see from the experimental data that for the higher pressures greater than 20 kbar, we can achieve pressures greater than 80% of those expected from the SESAME calculations, indicating that the fractional heat loss up until the peak of the pressure pulse in these cases is small. In this regime, therefore, we have a clear understanding of the plasma conditions, in terms of density, temperature, and internal energy, and little of the quartz confining wall has been vaporized. It can be seen from Fig. 5(b) that the predicted temperature of the plasma at 35 kbar from TFD SESAME calculations is about 17 eV, almost precisely the same as that produced by the method of x-ray heating of tamped foils outlined in the Introduction. In principle the plasma can also be probed by a separate optical or x-ray source. As the quartz confining walls are transparent down to just over 200 nm, the plasma can easily be probed with optical radiation through the walls. In the case of x-ray or extreme untraviolet (xuv) radiation, for which the quartz walls will be opaque, the plasma may be probed by displacing the two confining crystals laterally, as shown in Fig. 6, and coating the exposed surface of one of the crystals with the target material, as shown in the diagram. We have performed preliminary experiments which have shown that x rays can pass through the micrometer-scale gap, and can be recorded on a detector. It would thus be fruitful in the future to make further measurements of such a plasma, now that we have a good idea of its conditions.

In addition, by using this diffusion model, we also find that we can get qualitative agreement with the results of Fabbro *et al.* for their experiments where the initial metallic absorber is in intimate contact with the transparent confining wall. They showed that for their confined abla-

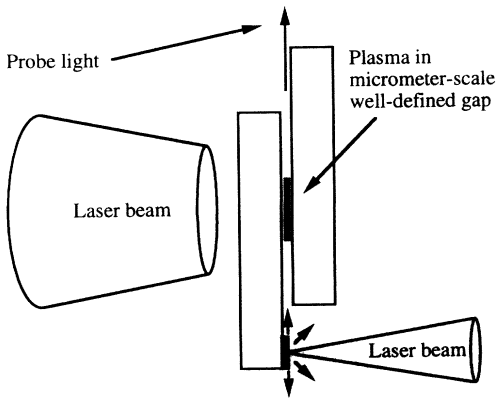

FIG. 6. A schematic diagram of a possible target design for x-ray probing of the confined plasma. Preliminary experiments have proved the feasibility of the design.

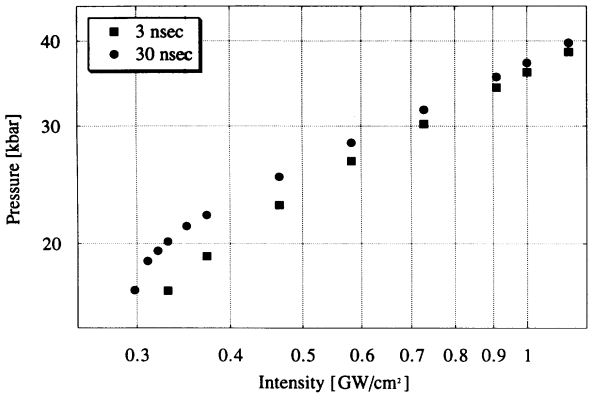

FIG. 7. The predicted peak pressure as a function of irradiance for the confined ablation case where the absorbing material is in intimate contact with the confining material. The peak pressure is calculated by solving Eqs. (1), (2), and (4) assuming a value of 2.49×10^{7} J m^{-2} s$^{-1/2}$ for $\beta\theta_m$. This figure should be compared with Fig. 7 of Ref. [15].

tion model, where the initial plasma thickness is negligible, the plasma pressure should be constant during a constant irradiance laser pulse, and should vary with intensity at $I^{1/2}$ [15]. Indeed, for long pulse lengths and high laser irradiances they found this dependence experimentally, as can be seen from Fig. 7 of Ref. [15]. However, at lower irradiances the pressure varied more strongly with irradiance, becoming approximately proportional to I. The transition from $I^{1/2}$ to I dependence took place at higher irradiances for shorter laser pulses. This general behavior is also predicted by the diffusion model given above. We have performed simulations for plasmas of very small initial thickness, as functions of irradiation and pulse length, using similar parameters to the work of Fabbro *et al.* The same diffusion constant of the 4 kbar shot shown in Fig. 4(a) was used throughout, and the results are shown in Fig. 7. The general form of the results is in good agreement with those observed by Fabbro *et al.* However, precise agreement with the observed pressures is not expected as the diffusivity could have been different in their experiments. In addition, the plasma produced by intimate contact between the absorbing surface and confining layer starts at a density close to solid and rapidly expands, thus changing rapidly in density throughout the laser pulse. It is not expected that α can be treated as a constant under such circumstances, and a more sophisticated model including SESAME equations of state may be required.

V. SUMMARY

In conclusion, we have presented a method of producing strongly coupled plasmas by the laser irradiation of thin metallic foils. This concept is an extension of previous methods of the production of strongly coupled plasmas by use of confined laser ablation. Thin (a few micrometers) plasmas can be produced with coupling parameters of order unity which may find application in the study of the equation of state and other properties of strongly coupled plasmas. As the plasmas are produced in well-defined micrometer-scale gaps, estimates of the ion density can be made, and thus comparisons can be drawn between experimental results and predictions for the equation of state of such strongly coupled plasmas. Initial measurements show that at low pressures (2–20 kbar) a significant fraction of the laser energy is lost due to thermal diffusion, whereas at higher pressures (20–35 kbar) this fraction decreases, and good agreement is found between the predictions of the SESAME equations of state and the experimental results. For all of the pressure range studied the peak pressures and the subsequent decay can be modeled using a very simple thermal diffusion model.

ACKNOWLEDGMENTS

We gratefully acknowledge the able help and support of the laser and target area staff of both the Janus and Vulcan laser systems.

[1] R. L. Shepherd, D. R. Kania, and L. A. Jones, Phys. Rev. Lett. **61**, 1278 (1988).
[2] G. R. Gathers, J. W. Shaner, and R. L. Brier, Rev. Sci. Instrum. **47**, 471 (1976).
[3] T. A. Hall, A. Djaoui, R. W. Eason, C. L. Jackson, B. Shiwai, S. J. Rose, A. Cole, and P. Apte, Phys. Rev. Lett. **60**, 2034 (1988).
[4] A. Ng, D. Parfeniuk, P. Celliers, L. DaSilva, R. M. More, and Y. T. Lee, Phys. Rev. Lett. **57**, 1595 (1986).
[5] D. R. Kania *et al.*, Phys. Rev. A **46**, 7853 (1992).
[6] W. Schwanda and K. Eidmann, Phys. Rev. Lett. **69**, 3507 (1992).
[7] L. B. DaSilva *et al.*, Phys. Rev. Lett. **69**, 438 (1992).
[8] L. C. Yang, J. Appl. Phys. **45**, 2601 (1974).
[9] R. J. Harrach, J. Appl. Phys. **47**, 2473 (1976).
[10] A. N. Pirri, Phys. Fluids **20**, 221 (1977).
[11] B. P. Fairand, B. A. Wilcox, W. J. Gallagher, and D. N. Williams, J. Appl. Phys. **43**, 3893 (1972).
[12] A. H. Clauer, B. P. Fairand, and B. A. Wilcox, Metall. Trans. A **8A**, 199 (1977); **8A**, 1872 (1977).
[13] N. C. Anderholm, Appl. Phys. Lett. **16**, 113 (1970).
[14] B. P. Fairand and A. H. Clauer, Opt. Commun. **18**, 588 (1976).
[15] R. Fabbro, J. Fournier, P. Ballard, D. Deveraux, and J. Virmont, J. Appl. Phys. **68**, 775 (1990).
[16] F. J. Mayer and G. E. Bush, J. Appl. Phys. **57**, 827 (1985).
[17] A. N. Mostoyvich, K. J. Kearney, J. A. Stamper, and A. J. Schmitt, Phys. Rev. Lett. **66**, 612 (1991).
[18] R. A. Graham, J. Appl. Phys. **32**, 555 (1961).
[19] R. A. Graham, J. Appl. Phys. **33**, 1755 (1962).
[20] R. A. Graham, F. W. Nielson, and W. B. Benedick, J. Appl. Phys. **36**, 1775 (1965).
[21] R. A. Graham and G. E. Ingram, J. Appl. Phys. **43**, 826 (1972).

[22] R. A. Graham, Phys. Rev. B **6**, 4779 (1972).
[23] R. A. Graham and L. C. Yang, J. Appl. Phys. **46**, 5300 (1975).
[24] SESAME Library, National Technical Information Service Document No. LA-7130 (B. J. Bennet, J. D. Jonhson, G. I. Kerley, and G. T. Rood, Los Alamos National Laboratory Report No. LA-7130, 1978). Copies may be ordered from the NTIS, Springfield, VA 22161.
[25] J. M. Hill and J. N. Dewynne, *Heat Conduction* (Blackwell Scientific, Oxford, 1987).

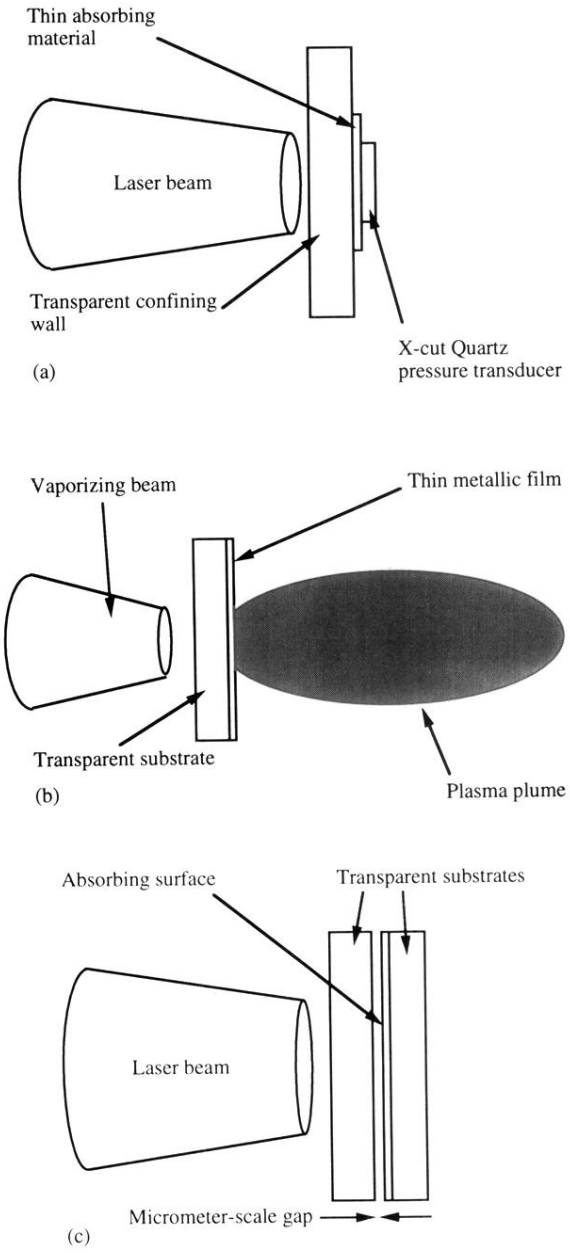

FIG. 2. A schematic diagram of the target design for confined laser ablation where (a) the absorbing surface is in intimate contact with the transparent confining wall; (b) where the absorbing film, irradiated from the side that is in contact with a transparent plate, is allowed to expand into the vacuum; and (c) irradiation of metallic foils which subsequently expand into a predefined micrometer-scale gap.

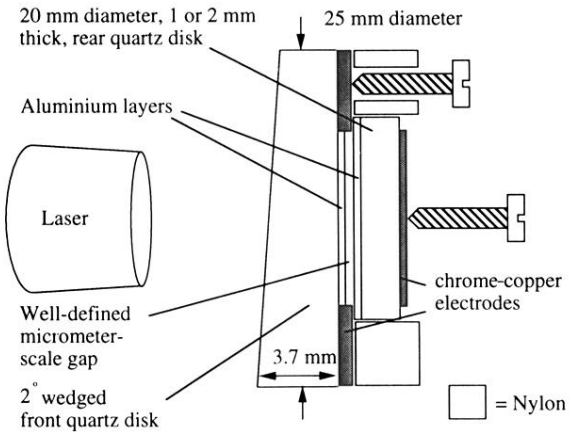

FIG. 3. A schematic diagram of the apparatus used to create the confined laser-produced plasma within a well-defined micrometer-scale gap.

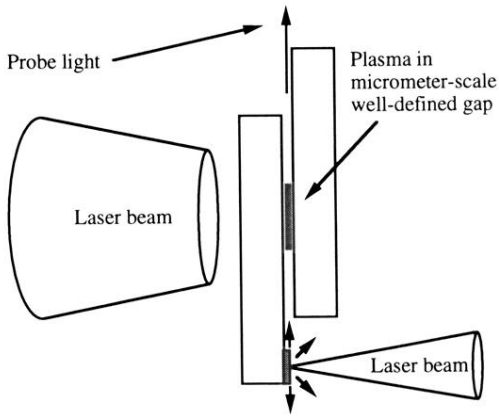

FIG. 6. A schematic diagram of a possible target design for x-ray probing of the confined plasma. Preliminary experiments have proved the feasibility of the design.